CFD '99
The International CFD Conference
5-7 June 1999 – Ulsteinvik, Norway

Investigation of Viscous Flow Around Modern Propulsion Systems

M. Abdel-Maksoud, H.-J. Heinke

SUMMARY

The in-homogeneity of the flow behind the ship and the high degree of turbulence increase the important for viscous flow effects on the performance of propellers and propulsion systems. Therefore, the interest of employing viscous flow methods for analysis and improving the efficiency of propulsion systems have been increased during the last years.

The paper describes the different procedures for simulation of the effect of the propeller action on the viscous flow. The capabilities and limitations of the procedures are demonstrated for different applications. Examples for viscous flow computations of the flow around propellers and propulsion systems are included. In the first example the flow behaviour in the tip vortex region of a propeller is investigated using numerical grids with different resolutions. The second example shows an investigation of the unsteady viscous flow on a ship arranged with a thruster. Viscous flow computations are also included for the flow around a pod-propulsion system and a double ended ferry with two azimuthing thrusters.

NOMENCLATURE

C_i	velocity vector in the inertial system
D	propeller diameter
e_{ijk}	permutation tensor
$_i$	index refer to the Cartesian co-ordinate direction *(i)*
$_j$	index refer to the Cartesian co-ordinate direction *(j)*
k	turbulent kinetic energy
$_k$	index refer to the Cartesian co-ordinate direction *(k)*
L_{PP}	length between perpendicular
P	pressure
t	time
U_i	velocity vector due to the rotation of the system
W_i	velocity vector relative to the rotating system
w_i	turbulent fluctuations
w_x	measured non-dimensional axial velocity component
w_t	measured non-dimensional tangential velocity component
w_r	measured non-dimensional radial velocity component
x_i	spatial co-ordinates
ε	dissipation rate of k
μ	molecular viscosity of the fluid
ρ	density
τ_{ij}	viscous stress tensor
ω_i	vector of system rotation

CFD '99
The International CFD Conference
5-7 June 1999 – Ulsteinvik, Norway

1. INTRODUCTION

Improving of the efficiency of modern ship propellers and propulsion systems requires detail information on the flow around the propulsors and the interaction parameters between propeller, appendages and ship hull. The inflow of the propeller effects the thrust distribution on the propeller blade. The induced velocities from the propeller effect also the inflow field. The interaction problem between the load distribution on the propeller blades and the propeller inflow behind the ship can be only investigated using an iterative procedure based on a viscous flow method. The application of the fully three-dimensional Reynolds-Averaged Navier-Stokes (RANS) techniques for analysing the flow around ship propellers for open water test condition was successfully applied by many research groups [1-3]. The propeller flow behind a ship form was investigated by [4]. The calculated effective wake field of a propeller was presented for different angular position of the propeller blades.

For propeller design, the effective wake field of the full scale is required. In the practice, a modified nominal wake field of the model is used. The employing of CFD-methods to calculate directly the effective wake field for full scale is still limited for special applications like naval and large passenger ships. With increasing the accuracy of numerical methods and the capacity of the computers it will be expected that CFD-methods will be applied for routine applications. The effect of the Reynolds number on the computed viscous flow results was investigated by many scientists [5-7]. The verification and validation of the full scale results will be an important subject for the ship hydrodynamic in the next years [8].

This paper describes the problem of computation of the flow around propulsion systems and ship-propeller configurations in the framework of the Reynolds-Averaged Navier-Stokes (RANS) equations. The purpose of the present study is not to present a grid converged solution of the propulsion problems, but to present some examples to demonstrate the applicability of numerical methods for the solution of such problems (technology demonstrator).

2. Numerical Method

For computation of the viscous flow around a ship with a propeller or a propulsion system including the propeller, the calculation domain is divided into a stationary part around the ship or the stationary part of the propulsion system and a rotating part around the propeller. In the first part a Cartesian co-ordinate system is employed. The flow around ship propellers is computed in a rotating co-ordinate system attached to the propeller. The RANS equations in a rotating co-ordinate system involve additional terms compared to those in an inertial system. The velocity vector in the inertial system can be divided into a velocity vector relative to the rotating system and the velocity vector due to the rotation of the system as follows:

$$C_i = W_i + U_i \tag{1}$$

Capital letters refer to time averaged variables. The speed of rotation is defined as:

$$U_i = e_{ijk} \varpi_j \chi_k \tag{2}$$

In this equation the permutation tensor e_{ijk} is used

$$e_{ijk} = \begin{cases} +1 \text{ for ijk cyclic,} \\ -1 \text{ for ijk anticyclic,} \\ 0 \text{ for ijk all other combinans.} \end{cases} \tag{3}$$

The equation for the conservation of mass reads:

$$\frac{\partial \rho}{\partial t} + \frac{\partial \left(\rho C_j \right)}{\partial \chi_j} = 0 \qquad (4)$$

The momentum equations in a rotating system are:

$$\frac{\partial \left(\rho C_i \right)}{\partial t} + \frac{\partial \left(\rho W_j C_i \right)}{\partial \chi_j} = - \frac{\partial P}{\partial \chi_i} - \frac{\partial \left(\tau_{ij} + \rho \overline{w_i w_j} \right)}{\partial \chi_j} - \rho e_{ijk} \omega_j C_k \qquad (5)$$

This form of the equations is optimal for the numerical simulation of flows with strong relative rotation between the co-ordinate system and the fluid [4]. The overbear refers to time averages of the turbulent variables. The viscous stress tensor is:

$$\tau_{ij} = - \mu \left(\frac{\partial W_i}{\partial \chi_j} + \frac{\partial W_j}{\partial \chi_i} \right) \qquad (6)$$

Since the density is constant for ship propeller flows, it is not necessary to solve an equation for the conservation of energy.

The effects of turbulence are modelled by the standard k-ε model [9]. Wall function boundary conditions are used.

The solution method is based on the conservative finite volume method CFX-TASCflow [10]. The code has been optimised and intensively tested within a joint research project between the Potsdam Model Basin GmbH and AEA Technology GmbH for different applications such as propeller in uniform flow and ship with rotating propeller flow [4]. The research project is founded by the German Ministry for Education, Research and Technology.

The numerical method includes fully conservative stage capabilities to simulate the interaction of the propeller with the propulsion system. The space discretisation is based on a block-structured finite volume grid around the propulsion system and the blades of the propeller. The grids at the interface between the rotating and the stationary frame do not have to match due to the capability of the code to handle general grid interfaces.

The next sections give a description of the application of the numerical method for simulation of propeller flows.

3. Simulation of propeller flows

The calculation of the viscous flow of propellers is a challenge for each numerical method. The difficulties are not only raised due to the complex geometry of ship propellers but also the complicated operation conditions. The viscous flow effects on the propeller performance are growing up with increasing the skew angle of the propeller blade, which is the case for modern ones. The advantage of application of viscous flow method is the consideration of the high level of turbulence in the wake field of the ship and the possibility of taking into account the interaction between the wake field of the ship and the propeller flow. Additional, the behaviour of the propeller flow in the different regions of the wake field can be analysed, specially the formation and developing of the tip vortex flow behind the propeller.

CFD ’99
The International CFD Conference
5-7 June 1999 – Ulsteinvik, Norway

For homogeneous inflow, the viscous flow calculation is carried out for one propeller blade and the interaction with the other propeller blades is taken into account using the periodically boundary condition. For the computation a rotating co-ordinate system is employed.

3.1 Application

Calculations of the viscous flow around propellers have become an important research field of the Potsdam Model Basin (SVA). Intensive research activities have been carried out in co-operation with AEA Technology during the recent years, in which the CFD method CFX-TASCflow has been used to study the details of the propeller flow. Now, the method is applied in many routine applications at SVA Potsdam. For validation of the numerical results, intensive LDV measurements were carried out in the cavitation tunnel of SVA, a description of the LDV measuring system at SVA can be found in [11]. The velocity field of different types of propellers were measured in detail, especially the flow around the blade tip. Figures 1, 2 and 3 show examples for the distribution of the axial velocity component at the plane x/D = 0.1 behind the propeller. Figure 2 and 3 include also the vectors of the tangential and radial velocity components. All information values were made dimensionless using the inflow velocity.

The measured results show the following characteristic flow regions:
- wake of the propeller blades,
- accelerated flow on the propeller blades mainly on the suction side,
- decelerated flow near the hub at the pressure side of the blade,
- highly accelerated flow within the tip vortex,
- highly decelerated flow within the tip vortex.

For the practice, it is important that the numerical method is able to predict the ship velocity at which the cavitation of the tip vortex begins and to estimate the pressure distribution in the centre of the tip vortex. The accuracy of the calculated pressure distribution is limited due to the complicated viscous effects and the very step gradients in this region. In the fact, the calculated minimum pressure at the centre of the tip vortex is strongly dependent on the resolution of the numerical grid.

This problem was investigated at Potsdam Model Basin (SVA) for a propeller, which was specially designed for this study. In contrary to the usual propeller design practice, the purpose of the propeller design in the present study was producing a good developed and stabile tip vortex.

A block-structured grid was applied. The computation was carried out for homogeneous inflow, therefore only one propeller blade was considered in the computation. The numerical grid consists of 7 blocks and includes 200 000 control volumes, see Figure 4. The computation was carried out for many advance coefficients. The presented results are for the advance coefficient of 1.245. To study the effect of the grid refinement on the numerical results, the numerical gird was refined in two steps. The region of tip vortex was refined with factor 3 and 9, see Figure 5. The first and the second refined grid include 279 000 and 1.5 million control volumes respectively.

The calculated velocity distribution behind the propeller is given in Figure 6. The calculated results show the same flow characteristic as the measured results in Figure 1.

Figures 7 and 8 show the effect of the grid refinement on the volume of the low pressure region. By increasing the refinement factor from 3 to 9, the calculated volume of the low pressure region is increased. The calculated value of minimum pressure was increased by about 50% percent and reached a value close to the vapour pressure of the water at the investigated test conditions.

Figures 9 and 10 show the calculated and the measured velocity components at non-dimensional propeller radius 0.94 and 1.0. The comparison between the measured and the calculated values shows a good agreement for the axial and radial velocity components and some differences for the tangential one.

4. Simulation of the flow around ship–propeller configuration

The traditional way of improving of the hull forms is the reducing of resistance of the bare hull. The recent developments on the field of numerical hydrodynamic allow the consideration of the effect of the propeller on the flow. In this case, it is possible to improve the hull form with respect to the delivered power. In some cases, the improving of a hull form from propulsion point of view alone can lead to increase the resistance of the bare hull, i. e. increasing the tunnel size of a tunnelled stern leads to increase the wetted surface area and also the possible diameter of the propeller. Depending on the individual case, the disadvantage of increasing the wetted surface area and the friction resistance of the ship can be more or less than the advantage of using larger propeller diameter. An accurate propeller model is needed to include the propeller characteristic into the viscous flow computation. The applied propeller models can be divided into three categories: steady, quasi-steady and unsteady. The selection of the suitable propeller model depends on the available time and the computational capacity for the numerical investigation. The different procedure for the simulation of the propeller effect in the flow will be discussed in the next sections.

4.1 Steady procedure

In the steady propeller model, the propeller is not directly considered but its effect on the flow at the propeller location. The function of the propeller as a propulsion organ is converting the delivered moment of the main engine into thrust. Due to the propeller action, the pressure and the axial velocity components are increased in the propeller plane. The moment of the propeller accelerates the flow in the circumferential direction, which causes the rotation of the propeller slipstream.

The simulation of the propeller effect on the flow is carried out using a three dimensional body force field [7, 12, 13]. The force distribution is a function of the radial distribution of the thrust and the moment of the propeller, which depends on the propeller geometry, inflow field of the propeller and the number of revolutions. In the viscous flow computation the body force distribution is assumed to be known and added directly to the source terms of the (RANS) equations. In the presented study, the actual thrust and moment distribution is estimated using a propeller performance method. The applied vortex lattice method VORTEX is able to handle every propeller geometry with an arbitrary radial inflow velocity distribution. The calculated thrust and moment distribution is averaged in the circumferential direction, so that the result is only a function of the non-dimensional radius of the propeller. A description of the applied vortex lattice method can be found in [14].

The calculated force distribution field is included in the numerical viscous flow calculation as external body force distribution. The forces are distributed in a disc with a finite thickness. The diameter of the disc is equal to the propeller diameter. The thickness is equal to the axial distance between the leading and the trailing edge of the propeller blades.

The flow in the stern region and the ship resistance are effected by the produced propeller thrust, due to pressure reduction in the front of the propeller. Therefore, the propeller thrust must be updated to consider the new inflow condition and the increased ship resistance. The computation is carried out in an iterative manner. After a certain number of iterations, the inflow to the propeller and the ship resistance are estimated in the viscous flow method and updated in the propeller performance method, which calculates the required propeller thrust and the corresponding moment and number of revolutions. After that, a new body force distribution is estimated and actualised in the viscous flow method.

The converged solution of the viscous flow computation includes not only the propeller effect on the flow at the propeller plane but also the propeller slipstream behind the propeller.

The advantage of this method is the short computing time. The computational effort is increased by about 15-20 % in comparison to the computation without propeller. The disadvantage of the method is that the accuracy of the calculated results is strongly depending on the accuracy of the propeller performance calculation method. Another disadvantage of employing steady treatment of the propeller model is the using of a disc with a finite thickness, which neglect the unsteady effects of the single blades on the flow.

4.2 Quasi-steady method

The real geometry of the propeller is considered in the viscous flow computation. Instead of using a propeller performance method the calculated pressure and wall shear stress distribution on the propeller blades are used to calculate the thrust and moment on the propeller blades. The computation of the viscous flow on the ship is carried out using a stationary co-ordinate system and on the propeller using a rotating one.

The numerical grid for the ship and for the propeller are separately generated. The grid generation for the propeller is a time consuming task due to the space limitation in the vertical direction between the ship bottom and the tip of the propeller and in the axial direction between the leading edge and the stern [4, 15].

The out shape of the numerical grid of the propeller has a cylinder form. The dimension of the cylinder is kept small as possible to allow the arrangement of the cylinder in the limited space at the propeller location behind the ship. The numerical grid of the ship is generated around the cylinder with the propeller grid and the ship form. For a single screw ship with propeller, the flow is asymmetric with respect to the symmetry plane, which means that the starboard and portside must be included in the computation. For a twin screw ship, only one ship side has to be considered in the computation due to the symmetry of the flow.

The idea of quasi-steady solutions is based on the assumption that for each angular position of the propeller a steady state solution is existed. Therefore, the solution is carried out for an angular position which is selected at the beginning of the computation. The information on connection between the faces of control volumes between the rotating and the stationary part of the numerical grid is determined one time at the beginning. The results of the computation are the pressure distribution on the ship and the propeller blades as well as the effective wake for the investigated angular position.

The advantage of the method is the simulation of the propeller flow in the viscous flow computation without using potential flow based assumptions. The disadvantage is the limitation of the results for one angular position and the high computational effort.

4.3 Unsteady method

The unsteady computation procedure is similar to the quasi-steady one, but the investigation is done for all angular positions in certain angular step normally between 4 and 5 degrees. In each time step the numerical grid of the propeller is rotated and the connection information between the rotating and the stationary part of the grid is recalculated. The unsteady calculations are started with a converged quasi-steady solution. The velocity and pressure distribution are available at each investigated angular position of the propeller.

In the next section some examples will be presented to show the capabilities of each propeller model for different applications.

4.4 Applications

4.4.1 Flow around a thruster with a ducted propeller

The propulsion systems manufacturer Schottel shipyard GmbH is well known for employing modern numerical and experimental methods for developing new products and improving existed ones. The propulsion system SRP 1212 of the company Schottel was investigated numerically and experimentally for bollard pull ahead condition. The aim of the investigation was the simulation of full scale tests. Therefore, the geometry of a towing tug boat is considered. The length, breadth and the draught of the tug are 32.5, 10.8 and 4.6 meter respectively. The numerical investigation was carried out for model and full scale. For model scale, the steady propeller model was applied. For full scale, the steady and the unsteady propeller models were employed.

A 3D solid CAD model was used for the grid generation. Special attention was given for every detail of the components of the rudder propeller and the propeller geometry as well as the ship. Three different numerical grids were employed, two for the steady propeller model, one for model scale and one for full scale. The third one was for the unsteady propeller model full scale.

For the steady computation, the numerical grid of the propeller part is modelled by disc with a finite thickness. For the unsteady one, the geometry of all propeller blades was considered without simplification. The clearance between the tip of the propeller blades and the nozzle is considered in the computation with steady and unsteady propeller model.

The length of the calculation domain was 2.75 L_{PP}, 0.75 L_{PP} in the front of the ship and one ship length behind it. The depth and the width of the calculation domain were equal to one ship length.

A block-structured grid was employed. The numerical grid for the steady propeller model consists of 70 blocks and 460 000 control volumes for model scale. The resolution of the numerical grid for the full scale in the near wall region is higher, the numerical grid contains 76 blocks and 530 000 control volumes.

For the unsteady propeller model, the number of used block is increased to 94. The total number of control volumes is 627 779. The numerical grid on the stern of the ship and the thruster with a ducted propeller is shown in Figure 11.

Figure 12 shows the contours of the axial velocity component on a longitudinal section through the thruster. For bollard pull condition, the numerical results are strongly depending on the simulation time of the computation. Figure 12 shows the results after 2 seconds simulation time. The length of the propeller slipstream is grown with increasing the simulation time. As a convergence criterion, it was assumed that a convergence is achieved, when the length of the propeller slipstream at least equals three times of propeller diameter.

The convergence behaviour of the numerical calculation is very sensitive to the applied boundary conditions for simulation of bollard pull ahead at the beginning of the computation. The investigation was started with inflow velocity equal to 0.1 m/s and after some iteration the inflow velocity was reduced to 0.0 m/s. The applied time step had to be kept very small to maintain the stability of the numerical computation. The achieved numerical results show many interesting aspects of the interaction between propeller, nozzle and housing.

4.4.2 Electric podded drive

The rapid growth of the market of podded propulsion systems encourages the manufacturers of propulsion systems to develop new products and to use advanced CFD-method to optimise the new systems.

The well known propeller manufacturer LIPS BV and STN ATLAS Marine Electronics GmbH have developed an advanced concept for the new podded propulsion system DOLPHIN. Extensive numerical and experimental investigations were carried out to support the development of the system.

The aim of the numerical investigations was the evaluation of the design of the strut and gondola from the hydrodynamic point of view and the estimation of the interaction parameter between propeller and housing. The numerical results were used to support the Reynolds number correction by offering detail information on the forces acting on the different parts of the system and the local velocity distribution. The investigation was carried out for model scale for several degrees steering angles. The steady propeller model was employed. The model considers the acceleration of the flow in the axial and circumferential direction. To simulate the correct inflow direction, the ship bottom of a twin screw ship was considered in the computation. The pod was mounted parallel to the ship bottom. The inclination angle in the longitudinal direction was about 5 degrees.

Different block-structured numerical grids were employed for different steering angles. For example, at 0 and 5 degrees steering angles, the computational domain was divided into 85 blocks, while the number of control volumes was about 500 000. The grid resolution was increased in the region between the strut and gondola and between the propeller and the pod. The rotation direction of the propeller was right handed. The 5 degrees steering angle was taken in the starboard direction.

Figure 13 shows the calculated streamlines around the pod by 5 degrees steering angle. The acceleration of the axial velocity component takes place more in the region below the gondola. In comparison with the measured data, the ratio of the calculated resistance of the pod to the produced thrust was quit good predicted. Figure 14 shows the axial velocity contours behind the podded propulsion system by 0 degrees steering angle. The contours of the velocity are symmetric in the region below the rotation axis and asymmetric in the region directly behind the strut. By non-zero steering angle, the velocity contours at the same plane are asymmetric in both regions.

4.4.3 Double ended ferry

The Potsdam Model Basin has started a research project on the optimisation of double ended ferries arranged with z-drive systems. The research project is supported by the German Ministry of Economy. A ship form is selected to be the basic form for the investigation. The basic ship form is a conventional one which is arranged with deadwood, see Figure 15. The propulsion system of the ship consists of two z-drive units for the bow and the stern region.

The computation of the viscous flow was carried out for the model scale with and without propeller. The steady propeller model is used in the computation. The propeller loading was the same for both propellers. The acceleration of the propeller flow was considered in the axial and circumferential directions. After evaluation of the numerical results, the ship form was modified to improve the propulsion and course stability of the ship. The new form is a completely tunnelled one.

The consideration of the rotation of the propeller slipstream behind the ship increases the number of control volume for calculation of ship flow by factor two in comparison with only considering the acceleration of the propeller slipstream in the axial direction. A block-structured grid is applied. Figures 16 and 17 show the topology of the numerical grid. The boundaries of propeller grid can be seen as disc in the front and

behind the ship. The body force distribution was added in these blocks. The total number of the employed control volumes was about 450 000.

The location of the propeller in the front of the ship effects the performance of the propeller and the flow around the ship in different ways. The inflow of the front propeller is nearly undistributed. The propeller slipstream dominates the flow on the forward part of the ship and leads to increase the velocity and

pressure. In comparison with the case without propeller, the resistance was increased by about 15 %. Beside increasing the ship resistance, an asymmetric pressure distribution takes place on the forward part of the ship.

The axial wake component in the propeller plane of the basic form is shown in Figure 18. The flow behind the ship without propeller is as expected symmetric. With operating propeller, the flow is accelerated more on one side of the ship than the other one, see Figure 19. The different pressure distributions on the both sides of the ship induce a transverse force. The estimated acting force on the forward half of the ship is about one third of the viscous resistance of this part. For the aft, the estimated one is much smaller. It is only about 6 % of the viscous resistance of the after half of the ship. Both forces are acting in the opposite direction, which produces a yaw moment. This moment is proportional to the propeller loading and has a strong influence on the course stability of the ship. The deadwood zone in the forward region of the ship is the most effected area from the asymmetric pressure distribution. Therefore, increasing the area of the deadwood has only a negative influence on the course stability of the ship.

According to the numerical results, the ship form was modified. The aim of modification was the reduction of the interaction between propeller slipstream and ship flow hull specially the from propeller induced side force. A completely tunnelled ship form was selected. This form has the advantage that the effect of the propeller slipstream is limited to the tunnel region, see Figure 20. The new ship form has the same displacement as the basic form but the wetted surface area is increased by 6.9 %. In comparison to the basic ship form, the resistance of modified from is 14.8 % higher without propeller and 3.6 % higher with propeller. The transverse force is totally disappeared. It is reduced from 30% to about 0.06 percent of the resistance of the forward part of the ship. For the after from, it is also reduced from 6% to 0.1 %.

Another advantage of the new hull form is the nearly homogeneous inflow of the aft propeller. This can be achieved in this case that the propeller and the ship can be considered as a one system. The calculated acceleration of the flow of the forward propeller should be nearly equal the reduction of the flow velocity due to the friction losses along the ship bottom. In this case, nearly similar inflow for forward and the aft propeller can be achieved, which improves the conditions to be meet for the optimisation of propeller geometry. The results show that a successful improving of the hull form can be only carried out when the propeller effect is taken into account. It is important to reduce the installed power of the main engine and not to reduce the resistance of the bare hull.

5. CONCLUSIONS

The application of CFD-method for analysing the flow around propulsion systems has become a routine application in Potsdam Model Basin. The advantage of CFD-analysis is providing of detail information on the flow such as the velocity and pressure distribution at each point in the computational field as well as the forces on each part of the propulsion system.

The consideration of the propeller effect on the flow can be carried out using different propeller models. The capabilities and limitation of the propeller models are discussed. The most advanced propeller model is the unsteady one. The interest of employing the unsteady propeller model for industrial application has been increased. The development of modern propulsion system can be effectively carried out by combining the unsteady propeller model with model tests.

Numerical investigations of the ship flow with working propeller provides detail information on the hull propeller interaction parameters. The consideration of the propulsion characteristic in the CFD-analyse of a hull form can lead in many cases to another results than by only investigating the bare hull form. The steady propeller model is able to capture the most important effects for the propeller effect in the first stage of the CFD-analysis. For the final one, the unsteady propeller model is recommended.

6. REFERENCES

/1/ Abdel-Maksoud, M., Menter, F. R., Wuttke, H.: Viscous Flow Simulations for Conventional and High Skew Marine Propellers, Ship Technology Research, Vol. 45, No. 2, 1998

/2/ Chen, B. , Stern, F.: Computational Fluid Dynamics for Four-Quadrant Marine Propeller, Proceeding of FED'98, FED SM 98-4872, ASME, 1998

/3/ Hsiao, C. T., Pauley, L. L.: Numerical Computational of Tip Vortex Flow Generated by a Marine Propeller, Proceeding of FED'98, FED SM 98-4871, ASME, 1998

/4/ Abdel-Maksoud, M., Menter, F. R., Wuttke, H.: Numerical Computation of the Viscous Flow around the Series 60 C_B = 0.6 Ship with Rotating Propeller, 3rd Osaka Colloquium on Advanced CFD Applications to Ship and Hull Form Design, Osaka, May 1998

/5/ Watson, S. J., Bull, P. W.: The Scaling of High Reynolds Number Viscous Flow Predictions Using CFD Techniques , 3rd Osaka Colloquium on Advanced CFD Applications to Ship and Hull Form Design, Osaka, May 1998

/6/ Eca, L., Hoekstra, M.: Numerical Calculation of Ship Stern Flow at Full-Scale Reynolds Numbers, Proceedings of 21st Symposium on Naval Hydrodynamics, Trondheim, Norway, June 1996

/7/ Tzabiras, G. D.: A Numerical Study of Additive Bulb Effects on the Resistance and Self-Propulsion Characteristic of Full Ship Form, Ship Technology Research, Vol. 44, 1997

/8/ L. Larsson, B. Regnström, L. Broberg, D-Q Li, C-E Janson: Failures, Fantasies and Feats in the Theoretical/Numerical Prediction of Ship Performance, 22nd Symposium on Naval Hydrodynamics, Washington DC, Aug. 1998

/9/ Launder, B. E., Spalding, D. B.: The Numerical Computation of Turbulent Flows, Comp. Meth. Appl. Mech. Eng., Vol. 3, pp. 269-289, 1974

/10/ Raw, M. J.: A Coupled Algebraic Multigrid Method for the 3D Navier-Stokes Equations in Fast Solvers for the Flow Problems, ed. W. Hackebusch, G. Wittum, Notes on Numerical Fluid Mechanics, Vol. 49, 1995

/11/ Mach, K. P.: LDA Geschwindigkeitsmessungen am Kavitationstunnel, 3. Fachtagung Lasermethoden in der Strömungsmeßtechnik, Bremen, Sept. 1994.

/12/ Stern, F., Kim, H. T., Zhang, D. H., Toda, Y., Kerwin, J., Jessup, S.: Computation of Viscous Flow Around Propeller-Body Configurations: Series 60 C_B = 0.6 Ship Model, Journal of Ship Research, Vol. 38., No. 2, 1994

/13/ Abdel-Maksoud, M., Rieck, K., Hellwig, K.: Numerical calculation of the induced velocities of a self propulsed inland vessel on a river bed, Euromech 374, Poitiers, April 1998

/14/ Bertolo, G., Brighenti, A., Kaul, S., Schulze, R.: LIUTO Development and Optimisation of the Propulsion System; Study, Design and Tests, 7th Int. Symposium on Practical Design of Ship and Mobile Units PRADS, The Hague, Sept. 1998

/15/ Menter, F. R., Abdel-Maksoud, M., Galpin, P.: Numerical and Modelling Aspects of Flow Simulations in Rotating Machines, Proceeding of FED'98, FED SM 98-5002, ASME, 1998

7. ACKNOWLEDGEMENTS

The authors would like to thank the German Ministry for Economic and the German Ministry for Education, Research and Technology for supporting the research projects on the field of application of CFD-methods for developing modern propulsion systems at Potsdam Model Basin. The authors would like also to thank the companies Schottel shipyard GmbH and LIPS BV for the good co-operation and the kind agreement for publishing some results of the numerical investigation, which were carried out at SVA Potsdam.

CFD '99
The International CFD Conference
5-7 June 1999 – Ulsteinvik, Norway

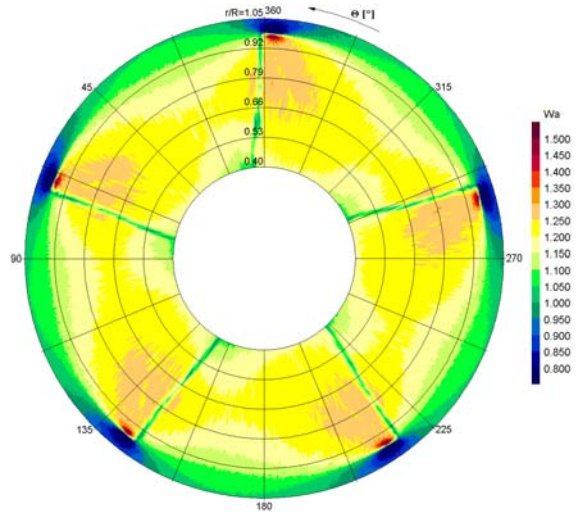

Velocity field measurements behind a model propeller x/D = 0.1

Figure 1: Distribution of the axial velocities

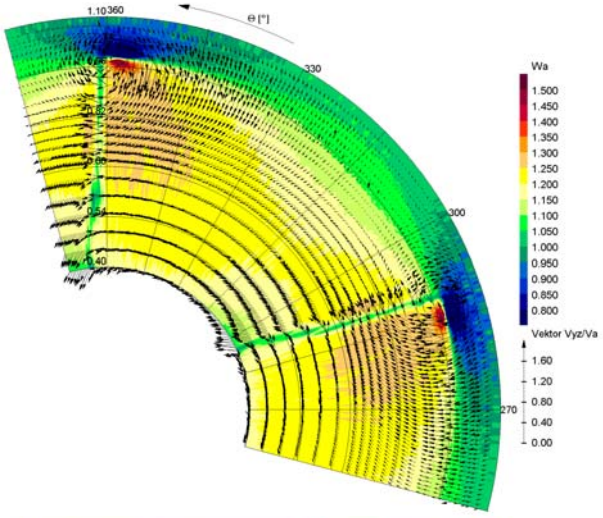

Figure 2: 3-dimensional velocity field

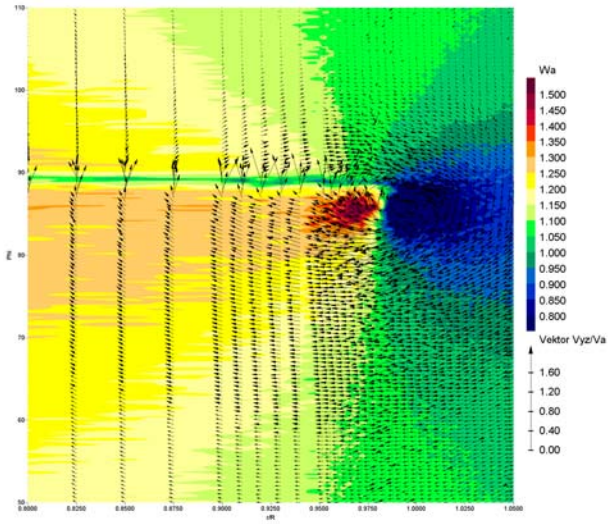

Figure 3: Flow field near the blade tip

CFD '99
The International CFD Conference
5-7 June 1999 – Ulsteinvik, Norway

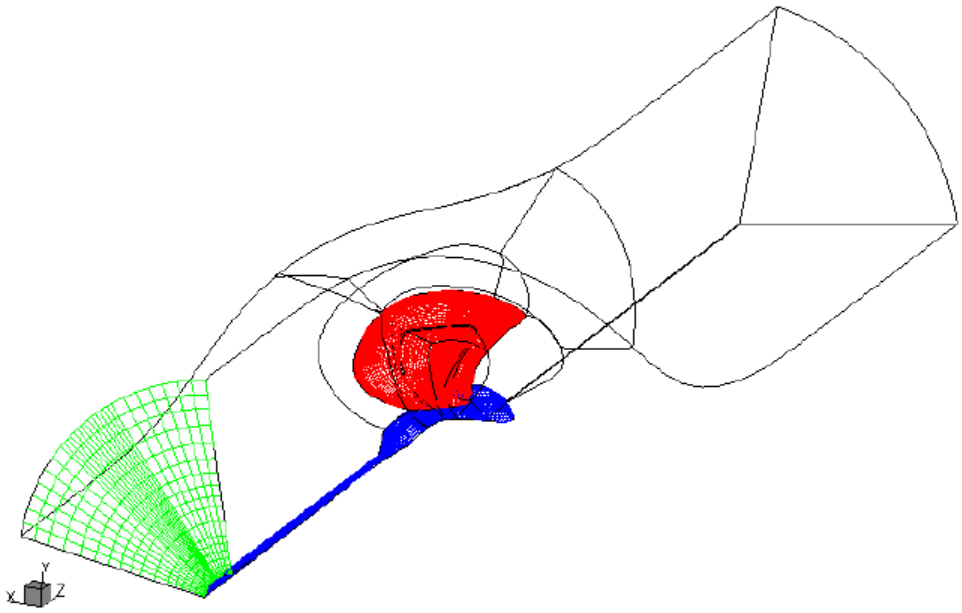

Figure 4: Topology of the numerical grid around the propeller blade

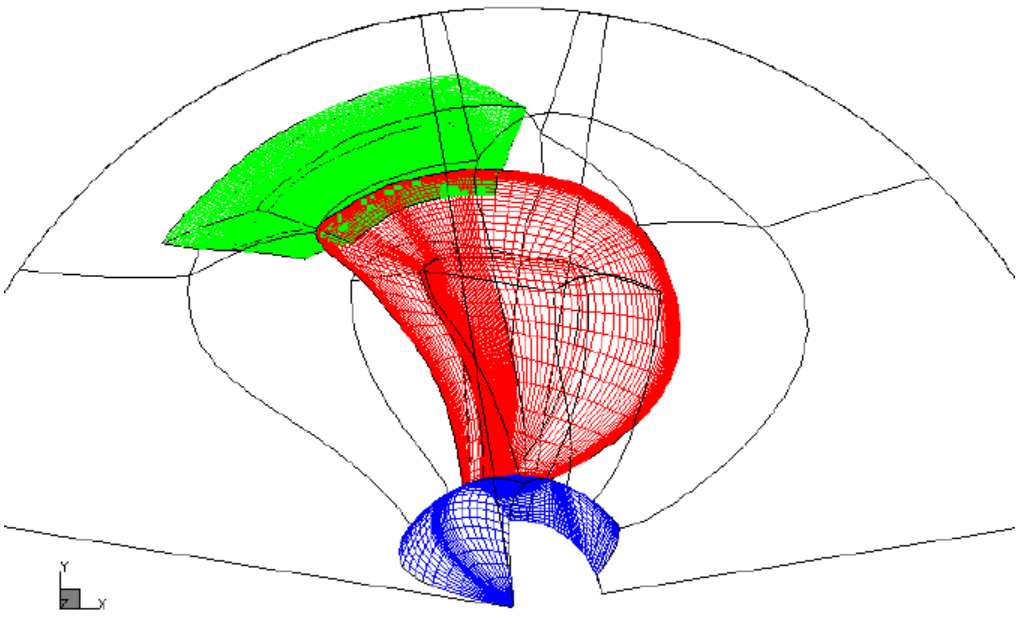

Figure 5: Region of local refinement near the tip of the propeller blade

CFD '99
The International CFD Conference
5-7 June 1999 – Ulsteinvik, Norway

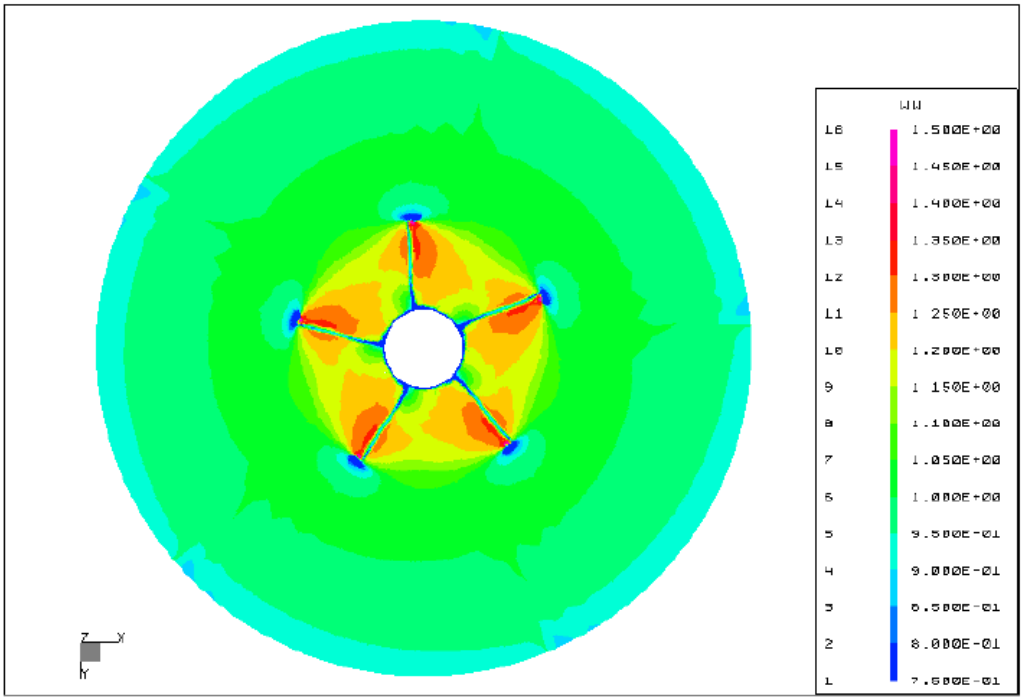

Figure 6: Calculated distribution of the axial velocity contours 0.1D behind the propeller

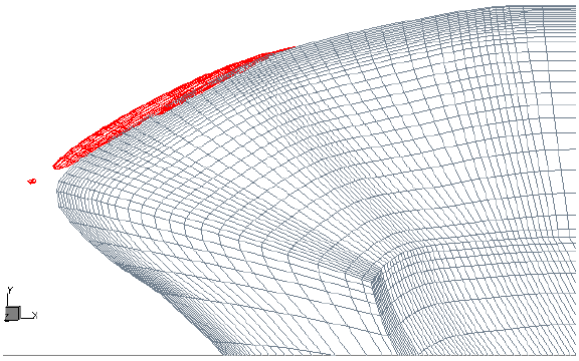

Figure 7: Low pressure region, refinement factor 3

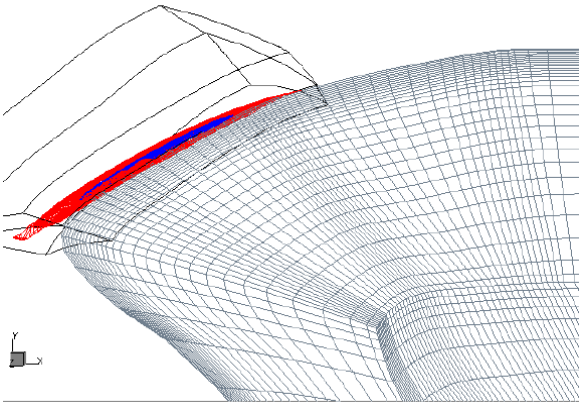

Figure 8: Low pressure region, refinement factor 9

CFD '99
The International CFD Conference
5-7 June 1999 – Ulsteinvik, Norway

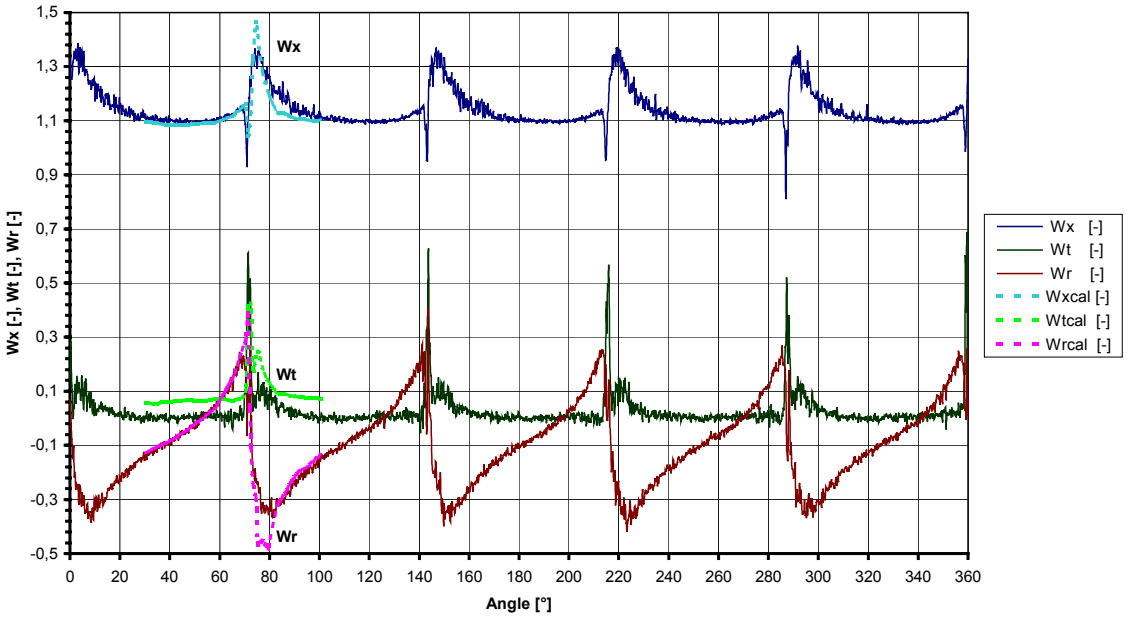

Figure 9: Measured and calculated velocities at x/D = 0.1, r/R = 0.95

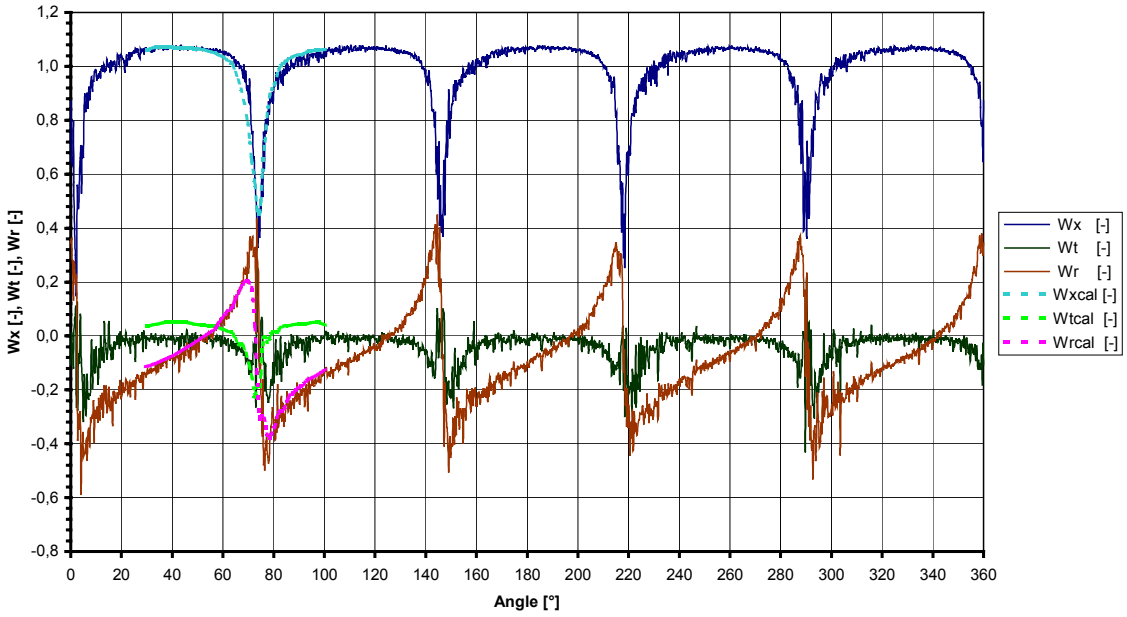

Figure 10: Measured and calculated velocities at x/D = 0.1, r/R = 1.00

CFD '99
The International CFD Conference
5-7 June 1999 – Ulsteinvik, Norway

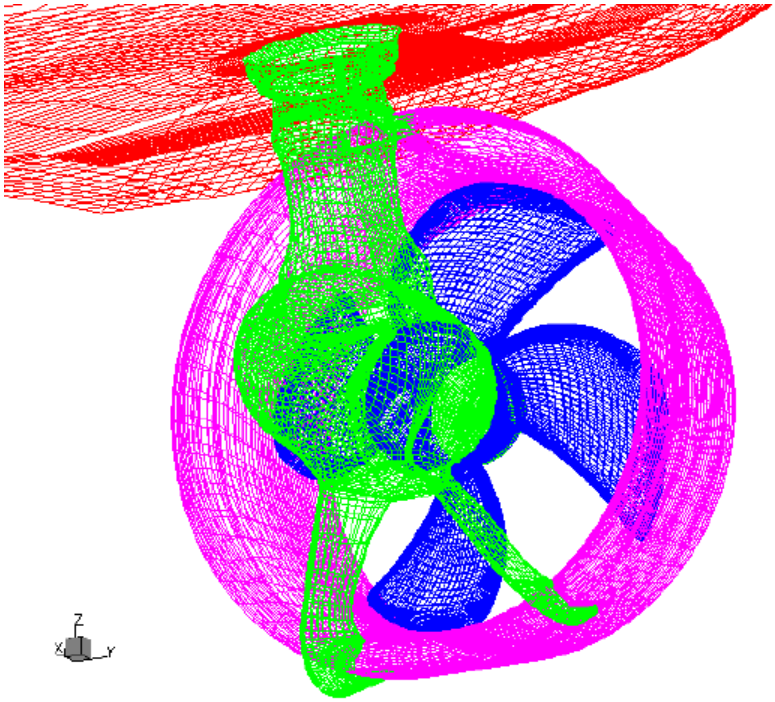

Figure 11: Numerical grid of the stern with thruster

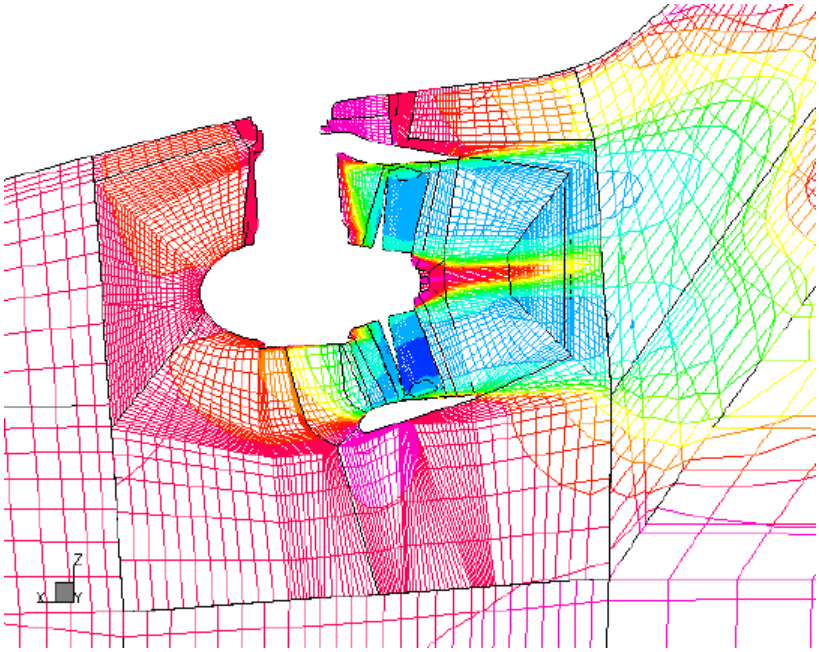

Figure 12: Axial velocity distribution in a longitudinal section through the thruster

CFD '99
The International CFD Conference
5-7 June 1999 – Ulsteinvik, Norway

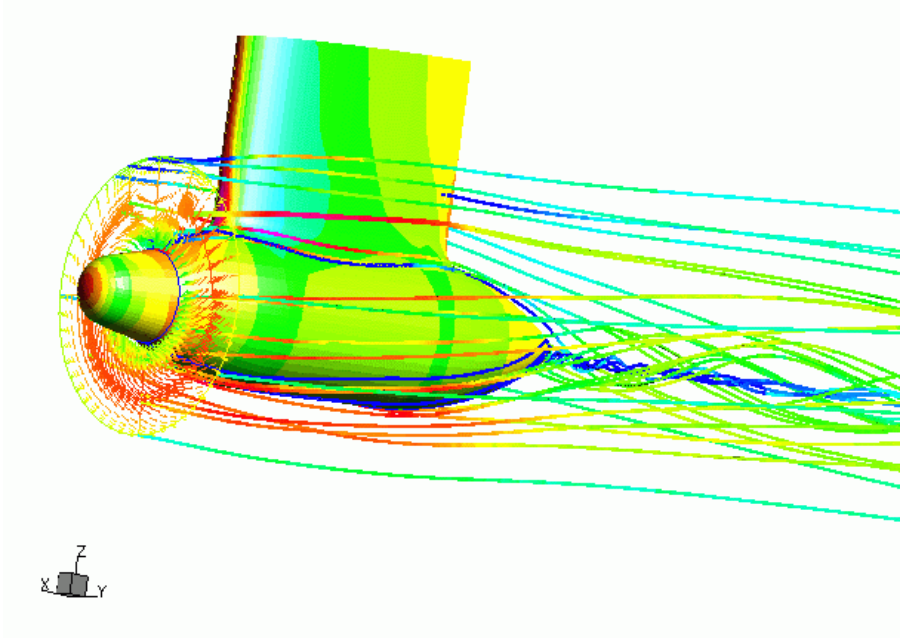

Figure 13: Velocity streamlines around the pod (steering angle 5°)

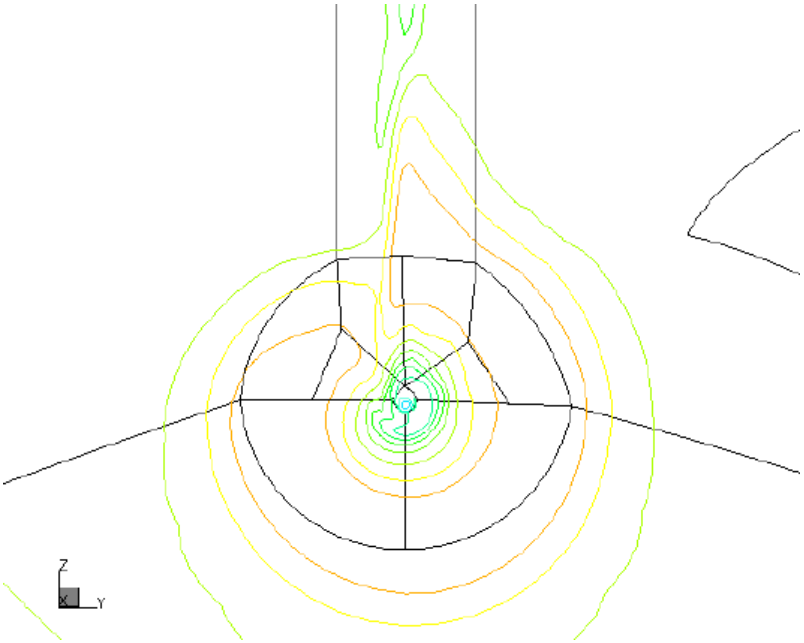

Figure 14: Velocity contours behind the trailing edge of the pod (steering angle 0°)

CFD '99
The International CFD Conference
5-7 June 1999 – Ulsteinvik, Norway

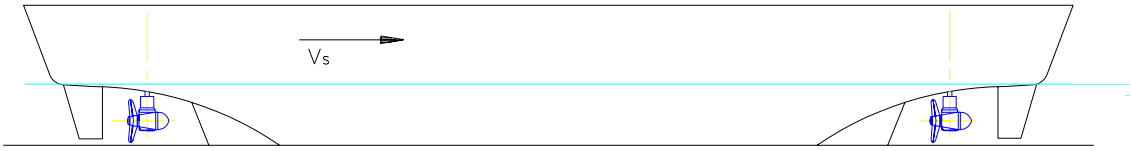

Figure 15: Double ended ferry with two azimuthing thrusters

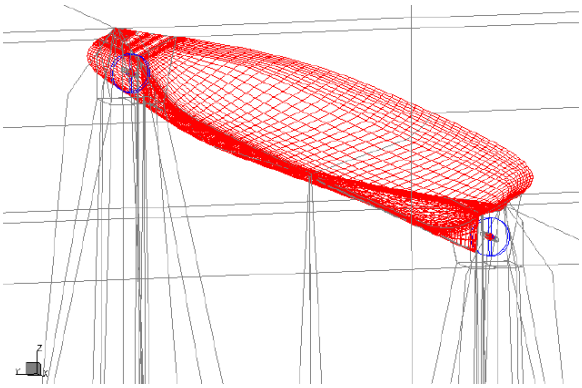

Figure 16: Numerical grid for the basic hull

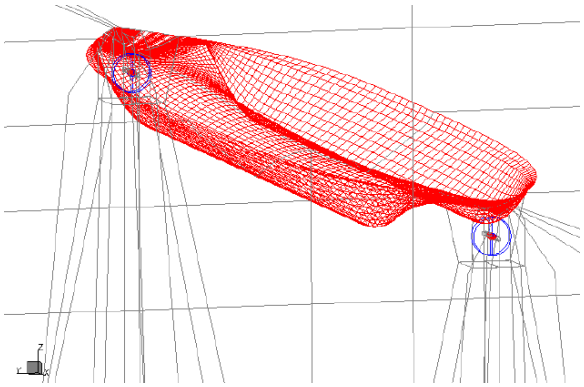

Figure 17: Numerical grid for the modified hull

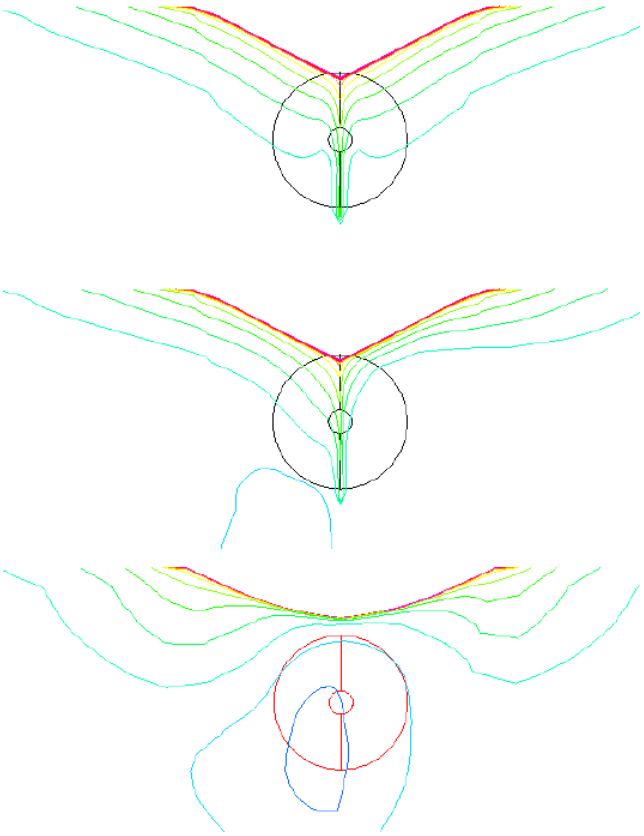

Wake field in the propeller plane of the aft z-drive

Figure 18: basic hull, without working forward z-drive

Figure 19: basic hull, with working forward z-drive

Figure 20: modified hull, with working forward z-drive